PHYSICAL REVIEW D VOLUME 17, NUMBER 5 1 MARCH 1978

$Q^2\bar{Q}^2$ resonances in the baryon-antibaryon system

R. L. Jaffe
Center for Theoretical Physics, Laboratory for Nuclear Science and Department of Physics, Massachusetts Institute of Technology, Cambridge, Massachusetts 02139
(Received 1 September 1977)

Two-quark–two-antiquark mesons which couple strongly to baryon-antibaryon channels are classified. The quantum numbers and masses of prominent states are predicted from the MIT bag model. The couplings of $Q^2\bar{Q}^2$ states to $B\bar{B}$ are estimated using the $^3P_0$ model and peripherality. Though most $Q^2\bar{Q}^2$ states do not couple strongly to $B\bar{B}$, many prominent resonances remain. Important $Q^2\bar{Q}^2$ resonances in the following processes are enumerated and discussed: elastic $N\bar{N}$ scattering, $N\bar{N}\to\pi^+\pi^-$, $N\bar{N}$ resonances at or below threshold, and exotic isotensor baryon-antibaryon resonances.

I. INTRODUCTION

The intent of this paper is to provide a framework for a quark-model classification of the many two-quark–two-antiquark ($Q^2\bar{Q}^2$) resonances expected to couple strongly to baryon-antibaryon channels. Many resonances are now known in the $B\bar{B}$ system[1], many more are to be expected. In meson-meson channels the quark model has provided a simple and successful classification scheme for resonances, assuming the resonances, like the mesons, to be $Q\bar{Q}$ states. The resonances lie on a few prominent Regge trajectories which are developed from ground-state $Q\bar{Q}$ configurations by the addition of angular momentum. The major roadblock to the analogous program in the $Q^2\bar{Q}^2$ sector is the sheer number of states. Here we will catalogue the $Q^2\bar{Q}^2$ trajectories, estimate their slopes and intercepts, and the relative strength with which they couple to $B\bar{B}$. Fortunately the vast majority couple only weakly. Our approach is, of necessity, rather eclectic. We use the bag model[2] to estimate slopes and intercepts. To estimate $B\bar{B}$ couplings we enlist a version of the $^3P_0$ model of Colglazier and Rosner[3] and some ideas about the peripheral nature of resonance formation in $B\bar{B}$ channels.[4] The program is only partially successful—too many states remain for us to unambiguously assign known $B\bar{B}$ resonances to quark-model configurations (with the possible exception of the states seen in $N\bar{N}\to\pi^+\pi^-$).

It has long been expected that $Q^2\bar{Q}^2$ mesons should appear as prominent elastic resonances in baryon-antibaryon scattering.[5] This expectation is based on duality and the quark model, and is conveniently summarized by the Harari-Rosner diagrams[6] of Fig. 1. The similarity of the duality diagrams for meson-meson, meson-baryon, and baryon-antibaryon scattering has led many people to the conclusion that $Q^2\bar{Q}^2$ mesons should lie on exchange-degenerate Regge trajectories.[7]

Until recently it has been impossible to say much about the dynamics of the $Q^2\bar{Q}^2$ system. The absence of low-mass exotic mesons which could be classified as $Q^2\bar{Q}^2$ states seemed to imply that the $Q^2\bar{Q}^2$ sector of the quark model was fundamentally different from the $Q\bar{Q}$ and Q^3 sectors, and discouraged attempts to incorporate $Q^2\bar{Q}^2$ states in the conventional quark model. Generally, $Q^2\bar{Q}^2$ states were exorcised from the spectrum. Their reappearance in $B\bar{B}$ channels was viewed as something of an embarrassment for duality.

From the standpoint of the MIT bag model,[2,8] multiquark hadrons ($Q^m\bar{Q}^n$, $n+m>3$) and ordinary mesons ($Q\bar{Q}$) and baryons (Q^3) are described by the same dynamics. When the spectrum of S-wave $Q^2\bar{Q}^2$ mesons was calculated, a possible dynamical origin for the absence of low-mass exotics emerged[9]: Color- and spin-dependent forces lower the mass of nonexotic $Q^2\bar{Q}^2$ configurations and increase that of exotic configurations. Exotic S-wave $Q^2\bar{Q}^2$ states were found to be far above threshold for dissociation decays into two $Q\bar{Q}$ mesons, making them very broad, if indeed they are resonant at all.[10] The lightest nonexotic $Q^2\bar{Q}^2$ configuration—a flavor-SU(3) nonet—may be identified with the known scalar mesons.[11]

Johnson and Thorn[12] developed a picture of leading Regge trajectories in the bag model which encorporates $Q^2\bar{Q}^2$ trajectories. They showed that the model predicts asymptotically linear trajectories, and that the slope parameter α' can be calculated. Their picture of a state on the leading trajectory is very simple; as shown in Fig. 2 the bag is deformed. The quarks sit at the ends and are connected by color-electric flux. For very large angular momentum, nearly all of the angular momentum and energy is carried by the gluon flux. The slope α' is determined by the magnitude of the color flux which is in turn fixed by the "color charge" on either end. For ordinary mesons and baryons the color representation on either

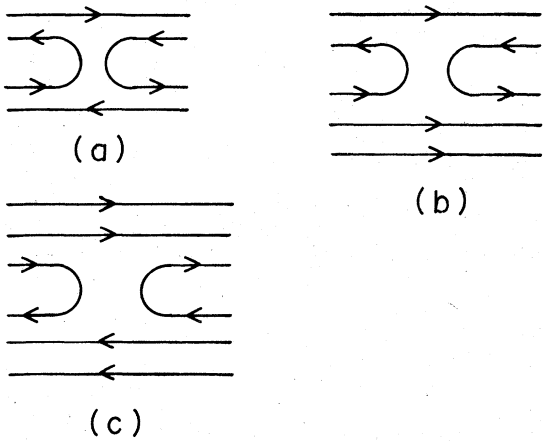

FIG. 1. Harari-Rosner diagrams for (a) meson-meson elastic scattering, (b) meson-nucleon elastic scattering, and (c) nucleon-antinucleon elastic scattering via a $Q^2\bar{Q}^2$ intermediate state.

end is always a $\underline{3}$ (or $\bar{\underline{3}}$), hence $Q\bar{Q}$ and Q^3 trajectories have the same slope, $\alpha' = 0.9\ \mathrm{GeV}^{-2}$.

Johnson and Thorn pointed out the implications of their work for $Q^2\bar{Q}^2$ trajectories. Two quarks may couple to a color $\bar{\underline{3}}$ or $\underline{6}$. Likewise a quark and and antiquark may form a $\underline{1}$ or $\underline{8}$. Thus three families of (overall color singlet) trajectories (with different slopes) are possible: $\bar{\underline{3}}$-$\underline{3}$, $\underline{6}$-$\bar{\underline{6}}$, and $\underline{8}$-$\underline{8}$. An important feature of this picture is that the $\bar{\underline{3}}$-$\underline{3}$ and $\underline{6}$-$\bar{\underline{6}}$ $Q^2\bar{Q}^2$ mesons are predominantly baryon-antibaryon resonances. Their coupling to purely mesonic final states is suppressed by an angular momentum barrier which is obvious from Fig. 3.

To estimate the masses of $B\bar{B}$ resonances we will combine the slope calculations of Johnson and Thorn with intercepts extracted from the s-wave masses of Ref. 9. First, however, it is necessary simply to enumerate all of the various $Q^2\bar{Q}^2$ trajectories. The number of possible arrangements of the spins, flavors, and colors of two quarks and two antiquarks is very large. Fortunately, not all couple strongly to baryon-antibaryon. Once the catalog is compiled it is straightforward to estimate the masses of $B\bar{B}$ resonances. All of this is presented in Sec. II. The catalog of $Q^2\bar{Q}^2$ trajectories may be found in Table III. As discussed in Sec. II, the mass estimates developed there must be regarded as rather crude.

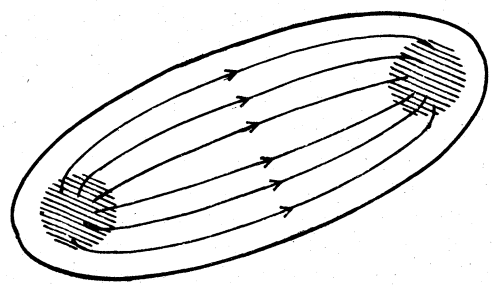

FIG. 2. A deformed bag. Separated color sources are linked by color–electric flux.

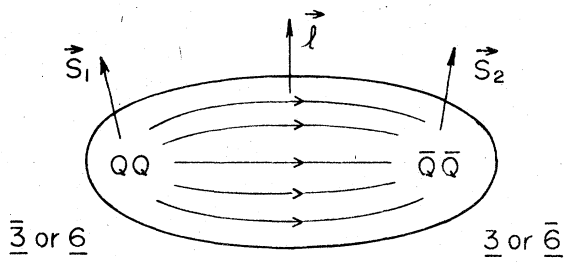

FIG. 3. A deformed $Q^2\bar{Q}^2$ state of the configuration expected to couple to $B\bar{B}$. Color representations and angular momentum vectors are shown.

The next objective is to estimate the relative strength with which important baryon-antibaryon channels couple to the various $Q^2\bar{Q}^2$ states. To do this we must develop a model for the reaction mechanism which couples $B\bar{B}$ to the $Q^2\bar{Q}^2$ states. This is discussed in Sec. III. We assume that the $Q\bar{Q}$ pair which annihilate carry vacuum quantum numbers, and that the nonannihilating quarks do not change their spin, color, and flavor configurations. This mechanism is conveniently summarized by the Harari-Rosner diagram [Fig. 1(c)], where the annihilating quarks just disappear and the spectators move on uninterruptedly. The same model has been used often in the literature to discuss ordinary meson and baryon decays.[3,13,14] The model enables us to calculate the relative coupling of any particular $Q^2\bar{Q}^2$ state to $N\bar{N}$, $N\bar{\Delta}$ (or $\Delta\bar{N}$), and $\Delta\bar{\Delta}$. (For simplicity we ignore strange and charmed quarks throughout this paper.) We find that certain $Q^2\bar{Q}^2$ trajectories couple very strongly to nucleon-antinucleon, while others couple very weakly. To learn more about $B\bar{B}$ couplings we introduce the notion of peripherality.[4] We assume resonance formation is peripheral and that the dominant partial wave is given by $L \approx kR$, where k is the center-of-mass momentum and R is a fixed interaction radius. Peripherality is a qualitative notion. We suppose only that states far from the peripherality curve are not likely to be prominent.

In Sec. IV we combine all these ingredients to study several baryon-antibaryon processes of particular interest: (1) Resonances in elastic $N\bar{N}$ scattering; (2) resonances in $N\bar{N} \to \pi^+\pi^-$; (3) $N\bar{N}$ resonances near or below threshold; (4) exotic isotensor baryon-antibaryon resonances. These exercises are performed primarily to illustrate the kind and quality of information contained in the catalog generated in Secs. II and III. In general we find that we are able to isolate a few promin-

ent trajectories in each case. As yet neither the theory nor experiment are precise enough to allow a unique identification of experimental effects with quark-model states ($N\bar{N}\to\pi^+\pi^-$ is a possible exception).

Many important effects still lie outside our quark-model dynamics. We cannot calculate the total widths of these $Q^2\bar{Q}^2$ resonances, nor the absolute widths into $B\bar{B}$. We have not attempted to study $Q^2\bar{Q}^2$-resonance formation in baryon [or antibaryon]-exchange processes such as $\pi^- p\to p_f$ $(p\bar{p}\pi^-)$. We have not studied trajectories built upon "radially excited" quark states, analogs of the ρ' trajectory in the $Q\bar{Q}$ sector. We expect these daughters to be less prominent than the ones we do study. We have not explored the relationship of our work to studies of the $B\bar{B}$ channel in the dual resonance model, topological expansion, etc.[15]

The reader will also note that we have not presented an argument that $Q^2\bar{Q}^2$ states dominate over $Q^3\bar{Q}^3$, $Q\bar{Q}$, or no-quark (pure gluon) states in the $B\bar{B}$ sector. We may exclude $Q^3\bar{Q}^3$ trajectories because they have very low intercepts. $Q^2\bar{Q}^2$ trajectories are not prominent in meson-meson scattering for the same reason. $Q\bar{Q}$ and gluon states are suppressed because they require more $Q\bar{Q}$ annihilations (Okubo-Zweig-Iizuka rule). A $Q\bar{Q}$ resonance in $B\bar{B}$ is analogous to a gluon resonance in meson-meson scattering (same number of annihilating $Q\bar{Q}$ pairs) for which there is little, if any, evidence. We expect gluon resonances in $B\bar{B}$ to be even more suppressed.

Since this paper is intended to be useful for experimentalists, we have tried to separate the model calculations from the useful results. The catalog of Sec. II and III is summarized in Tables III, V, and VI, which are reasonably self-contained. Tables I and II, and Figs. 3 and 4 provide an interpretive "key" to the catalog. The discussion of specific processes is confined to Sec. IV and to the Conclusion. A partial, qualitative account of this work was reported in collaboration with Johnson.[16]

II. CLASSIFICATION AND SPECTRUM OF $Q^2\bar{Q}^2$ RESONANCES

Quarks carry color, flavor, and spin quantum numbers. Color is, as usual, a gauged SU(3) symmetry which is assumed to be confined: All hadrons are color singlets. Since we are ignoring strangeness and charm, flavor reduces to the (assumed exact) SU(2) of isospin. What we call "spin" is actually the total angular momentum of a relativistic quark referred to the center-of-mass of a baryon or antibaryon. Since only quarks with angular momentum $\frac{1}{2}$ will occur in our work they may be described by the algebra of SU(2), allowing us to borrow the familiar terminology of spin.

The notion of "diquarks" will simplify our discussion immensely. Two quarks in the same spatial state must be antisymmetric under simultaneous exchange of color, spin, and flavor labels. If the quarks are antisymmetrized in color (the $\underline{\bar{3}}$ representation), they must be either symmetric in both isospin and spin ($i=s=1$) or antisymmetric in both ($i=s=0$). We denote these as δ and β "diquarks", respectively. If the quarks are symmetrized in color (the $\underline{6}$ representation) they may be either symmetric in spin and antisymmetric in flavor ($s=1, i=0$) or vice versa ($s=0, i=1$). We denote these as γ and α "diquarks", respectively. This notation is summarized in Table I.

The nucleon (N) and Δ SU(6) wave functions are particularly simple in terms of diquarks:

$$N=\frac{1}{\sqrt{2}}(\beta Q+\delta Q)^{(2,2)}, \tag{2.1}$$

$$\Delta=(\delta Q)^{(4,4)}, \tag{2.2}$$

where the superscripts denote the overall coupling of spin and isospin $(2S+1, 2I+1)$. Of course the three quarks are coupled to an overall color singlet. Notice that the color-symmetric diquarks do not appear in these (or any Q^3 baryon) wave functions.

Following Johnson and Thorn we describe a $Q^2\bar{Q}^2$ state with high angular momentum as follows: In a rotating frame the system is cigar shaped. On one end sit two quarks and on the other end sit two antiquarks. States in which a $Q\bar{Q}$ (color $\underline{8}$) pair sits on either end do not appear to couple to baryon-antibaryon and will not be considered further. The total angular momentum is composed of three terms, the angular momentum of the two quarks about their center-of-mass $\vec{s}_1$, the angular momentum of the two antiquarks about their center-of-mass $\vec{s}_2$, and the relative angular momentum of the quarks and antiquarks $\vec{l}$ (see Fig. 3). For fixed l, the energy of a state is minimized when the quarks (and antiquarks) are in the ground state of their relative motion. This is the "leading trajectory". For these states the two quarks may be characterized as a diquark and the two antiquarks as an

TABLE I. Diquarks: Allowed color, spin, and isospin configurations for spatially equivalent QQ systems.

Name	Color representation	Spin	Isospin
β	$\underline{\bar{3}}$	0	0
δ	$\underline{\bar{3}}$	1	1
γ	$\underline{6}$	1	0
α	$\underline{6}$	0	1

TABLE II. Definitions of quantum numbers

Quantum number	Definition
J	Total angular momentum
L	Orbital angular momentum in the $B\bar{B}$ channel
S	Spin in the $B\bar{B}$ channel
I	Total isospin
(S_1, I_1)	Spin and isospin of baryon
(S_2, I_2)	Spin and isospin of antibaryon
(s_1, i_1)	Spin[a] and isospin of diquark
(s_2, i_2)	Spin[a] and isospin of antidiquark
$\mathcal{S}$	Total spin[a] of diquark and antidiquark
l	Relative angular momentum of diquark and antidiquark

[a] Actually the total angular momentum relative to the baryon (or antibaryon) center of mass.

antidiquark. $B\bar{B}$ channels (where B is an N or Δ) should couple most strongly to these configurations since all quarks in the N and Δ are in the ground state.

The $Q^2\bar{Q}^2$ trajectories may be classified first according to their diquark-antidiquark content and then according to the total quark-spin ($\mathcal{S}$, which is the composition of s_1 and s_2) and isospin (I). We choose to label the position of a state on a trajectory by the relative angular momentum (l) rather than the total angular momentum (J) for reasons of convenience which will become apparent below. The definitions of these quantum numbers are summarized in Table II. For a given l and $\mathcal{S}$ there are actually a family of trajectories with J ranging from $|l-\mathcal{S}|$ to $l+\mathcal{S}$. The diquark content and quantum numbers of these $Q^2\bar{Q}^2$ resonances are listed in the first few columns of Table III. To illustrate the content of this table we have constructed the analogous table for the familiar $Q\bar{Q}$ trajectories. The first entry of Table IV, $(Q\bar{Q})^0$, includes η and π trajectories ($I=0, 1$). The second entry, $(Q\bar{Q})^1$, includes six trajectories. For each isospin, the quark spin couples to l to yield three different total angular momenta J. For $J=l+1$ we have the ω and ρ trajectories. For $J=l$ we have the "H" and B trajectories (the H is the yet-to-be-discovered isoscalar brother of the B). For $J=l-1$ we have the "ϵ" and "δ" trajectories (the ϵ and δ are isospin 0 and 1 scalar $Q\bar{Q}$ mesons which may or may not be identified with known scalar mesons). Exchange degeneracy is assumed.

TABLE III. Classification of $Q^2\bar{Q}^2$ trajectories in a diquark-antidiquark scheme. The parity of all states is $(-1)^l$. See Tables I and II for notation.

States (diquark content)	$\mathcal{S}$	J	I	G	Mass squared (GeV^2)
A: $\beta\bar{\beta}$	0	l	0	$(-1)^l$	$1.1l+1.62$
B^+: $(1/\sqrt{2})(\beta\bar{\delta}+\delta\bar{\beta})$	1	$l-1$ to $l+1$	1	$(-1)^{l+1}$	$1.1l+1.88$
B^-: $(1/\sqrt{2})(\beta\bar{\delta}-\delta\bar{\beta})$	1	$l-1$ to $l+1$	1	$(-1)^l$	$1.1l+1.88$
C: $(\delta\bar{\delta})^{\mathcal{S}=0}$	0	l	0,1,2	$(-1)^{l+I}$	$1.1l+2.40$
C: $(\delta\bar{\delta})^{\mathcal{S}=1}$	1	$l-1$ to $l+1$	0,1,2	$(-1)^{l+I+1}$	$1.1l+2.40$
C: $(\delta\bar{\delta})^{\mathcal{S}=2}$	2	$l-2$ to $l+2$	0,1,2	$(-1)^{l+I}$	$1.1l+2.40$
$\alpha\bar{\alpha}$	0	l	0,1,2	$(-1)^{l+I}$	$1.75l+2.56$
$(1/\sqrt{2})(\alpha\bar{\gamma}+\gamma\bar{\alpha})$	1	$l-1$ to $l+1$	1	$(-1)^{l+1}$	$1.75l+2.28$
$(1/\sqrt{2})(\alpha\bar{\gamma}-\gamma\bar{\alpha})$	1	$l-1$ to $l+1$	1	$(-1)^l$	$1.75l+2.28$
$(\gamma\bar{\gamma})^{\mathcal{S}=0}$	0	l	0	$(-1)^l$	$1.75l+2.02$
$(\gamma\bar{\gamma})^{\mathcal{S}=1}$	1	$l-1$ to $l+1$	0	$(-1)^{l+1}$	$1.75l+2.02$
$(\gamma\bar{\gamma})^{\mathcal{S}=2}$	2	$l-2$ to $l+2$	0	$(-1)^l$	$1.75l+2.02$

TABLE IV. Classification of $Q\bar{Q}$ trajectories in analogy to Table III.

States (quark content)	$\mathcal{S}$	J	I	G	Mass squared (GeV^2)
$(Q\bar{Q})^0$	0	l	0,1	$(-1)^{l+I}$	$1.1l$
$(Q,\bar{Q})^1$	1	$l-1$ to $l+1$	0,1	$(-1)^{l+I+1}$	$1.1l+0.59$

This method of classifying trajectories has several virtures:

(1) It is "natural" from the standpoint of the quark model. States on the π trajectory *are* described as orbital excitations of the pion.

(2) Nonsense zeroes and the like fall out automatically as consequences of the composition rules of angular momentum. There is, for example, no $J=0$ state on the ρ trajectory because $l+1\geq 1$ is guaranteed by angular momentum composition.

(3) Families of roughly degenerate states are grouped together. Quark-model fits to $Q\bar{Q}$ and Q^3 spectra indicate that masses depend strongly on l and on $\mathcal{S}$ but only weakly on J.

Returning to Table III, it is apparent that there are a vast number of $Q^2\bar{Q}^2$ trajectories. The first set of states in Table III are constructed from color-antisymmetric diquarks (β and δ); the second set are constructed from color-symmetric diquarks (α and γ) which will be seen not to couple strongly to $B\bar{B}$. Among the first class of states there are three general types which we have labeled A, B, and C. A-type states are composed of $\beta\bar{\beta}$ and have spin and isospin zero. B-type states are linear combinations (to diagonalize G parity) of $\beta\bar{\delta}$ and $\delta\bar{\beta}$ and have spin and isospin 1. The C type states are composed of $\delta\bar{\delta}$ and may coupled to $\mathcal{S}=0$, 1 and 2, and $I=0$, 1 and 2. The great majority of $Q^2\bar{Q}^2$ trajectories arise from the C-type configuration. Sorting out the couplings of the states in Table III is the subject of the next section.

We turn now to make estimates of the slopes and intercepts of the states listed in Table III. Johnson and Thorn[12] showed that for large l these states lie on exchange degenerate, linear Regge trajectories:

$$l=\alpha' M^2+\alpha_0, \tag{2.3}$$

and that the slope may be calculated in terms of the color charge which resides on either end of the bag:

$$1/\alpha'=4\pi(2\pi\alpha_c BC^2)^{1/2}. \tag{2.4}$$

Here B is the bag pressure and α_c is the fine-structure constant of quantum chromodynamics. C^2 is the eigenvalue of the quadratic Casimir operator for the color on either end. $B^{1/4}$ and α_c are determined by low-energy spectroscopy to be 146 MeV and 0.55, respectively. For a meson or baryon $C^2=\frac{16}{3}$, so that $\alpha'=0.88\ \mathrm{GeV}^{-2}$ in excellent agreement with the experimental value $0.9\ \mathrm{GeV}^{-2}$.

There are two families of Regge trajectories composed of diquarks and antidiquarks.[12] States with the color $\bar{3}$-3 configuration lie on trajectories with the same slope as ordinary $Q\bar{Q}$ and Q^3 trajectories, $\alpha'(\bar{3}\text{-}3)=0.9\ \mathrm{GeV}^{-2}$. For color 6-$\bar{6}$ configurations, $C^2=\frac{40}{3}$ and $\alpha'(6\text{-}\bar{6})=0.57$. The 6-$\bar{6}$ states are therefore more widely spaced in mass than the $\bar{3}$-3 states.

To estimate the intercepts of $Q^2\bar{Q}^2$ trajectories we must make contact with the calculations of s-wave $Q^2\bar{Q}^2$ states in Ref. 9. This program has several pitfalls, all having to do with the curvature of Regge trajectories. First, we do not know why $Q\bar{Q}$ and Q^3 trajectories should remain linear down to very low values of l. Though this is fundamental to the dual resonance model and seems to be true in nature we know of no strong argument for it in the bag model (or any other relativistic quark model). Second, even if the $Q\bar{Q}$ and $\bar{Q}^3$ trajectories remain linear down to $l=0$, there is reason to expect curvature in $Q^2\bar{Q}^2$ trajectories. The reason is that the S-wave $Q^2\bar{Q}^2$ states are linear combinations of color-symmetric diquarks and antidiquarks (6-$\bar{6}$) and color-antisymmetric diquarks and antidiquarks ($\bar{3}$-3).[9] The mixing is induced by color-magnetic interactions between the quarks and antiquarks. Color-magnetic forces split the N from the Δ and the π from the ρ in this model.[8] As angular momentum (l) is added to the system, the diquarks and antidiquarks separate, the color-magnetic interaction between them probably diminishes,[17] and the mixing disappears. The $\bar{3}$-3 and 6-$\bar{6}$ trajectories emerge as pure states. Mixing between $\bar{3}$-3 and 6-$\bar{6}$ trajectories at low l implies curvature in both. This phenomena cannot occur in the $Q\bar{Q}$ or Q^3 sectors.

We have incorporated this curvature as follows: First we assume that if the color-magnetic mixing is "turned" off, the $\bar{3}$-3 and 6-$\bar{6}$ trajectories would remain linear down to $l=0$, in analogy with the Q^3 and $Q\bar{Q}$ sectors. The intercept is given by $\alpha_0=-\alpha' M_0^2$, where M_0 is the expectation value in a pure $\bar{3}$-3 or 6-$\bar{6}$ state of the s-wave Hamiltonian of Ref. 9 with the $Q\bar{Q}$ color-magnetic interactions turned off.[18] The resulting linear mass formulas for $Q^2\bar{Q}^2$ trajectories are given in the right-hand column of Table III. It should be emphasized that these results are certainly not valid for $l=0$ where trajectories mix substantially. Although we may use the linear formulas of Table III in making rough estimates for l as low as 1 we expect curvature in $Q^2\bar{Q}^2$ trajectories for small l.

III. $Q^2\bar{Q}^2$ COUPLINGS TO $B\bar{B}$ CHANNELS

We assume that the coupling of $Q^2\bar{Q}^2$ states, such as the one shown in Fig. 3, to mesons is suppressed for large l. The argument is that meson decays require tunneling of a quark or antiquark through an angular momentum barrier. For small values of l the argument fails, and we expect large widths into purely mesonic channels. For $l=0$, meson channels surely dominate.[9] We will not discuss $l=0$ states further here. For higher l we believe $B\bar{B}$ channels dominate, but are unable to find a quantitative estimate of the relative importance of mesonic and $B\bar{B}$ channels. We have chosen a very simple model in which to calculate the coupling to $B\bar{B}$ channels: The annihilating $Q\bar{Q}$ pair are assumed to have vacuum quantum numbers ($J^\pi=0^+$, $I=0$, color singlet) and the nonannihilating quarks (or antiquarks) are assumed to remain in the same configuration (spin, flavor, and color) which they occupied in the incident baryon (or antibaryon). This model is known in the literature by many names, the $^3P_0$ model and the quark-pair creation model among others.[3,13,14] It provides a quite successful description of P-wave baryon and meson decays and is somewhat more general, though less predictive, than the Melosh approach.[14]

The first consequence of this model is that the entire family of $\underline{6}$-$\underline{\bar{6}}$ Regge trajectories decouple from the $B\bar{B}$ system. These are the states in Table III composed of α- and γ-type diquarks. Although rather obvious, this selection rule is extremely important. It eliminates half of the possible trajectories at one swoop making the classification problem more manageable.

Consider a particular resonance from Table III. It is described by the quantum numbers of the diquark and antidiquark (s_k and i_k, $k=1$, 2), and by l, s, J, and I as previously defined. When a $J^\pi=0^+$ $Q\bar{Q}$ pair is created, the Q (or $\bar{Q}$) has some amplitude to be in the ground state relative to the pre-existing diquark (or antidiquark). This is the only piece of the amplitude which concerns us (the rest of the amplitude describes the coupling of the $Q^2\bar{Q}^2$ system to excited baryon-antibaryon channels). It is certain to be l-dependent. Therefore we are unable to relate the coupling of $Q^2\bar{Q}^2$ states with different l. Also, a given $Q^2\bar{Q}^2$ state will often be found to couple to more than one partial wave in the $B\bar{B}$ system. This is familiar from the original application of the $^3P_0$ model to the decay $B\to\omega\pi$ in which both S and D $\omega\pi$ waves can contribute. The relative importance of S and D waves depends on much more than naive angular momentum couplings. Following Colglazier and Rosner we will leave the couplings to different partial waves free. The model assumes that the only dependence of the amplitude on s, S, I, and J is that required by the recoupling of spins, isospins, and angular momenta in going from the initial $Q^2\bar{Q}^2$ state to the final $B\bar{B}$ channel.

The model is very predictive. The basic vertex is shown in Fig. 4. Note the quantum numbers of the created $Q\bar{Q}$ pair: $J^\pi=0^+$ requires $l=s=1$. Certain selection rules are immediate. First,

$$L=l\pm1, \tag{3.1}$$

$L=l$ is forbidden by parity; second

$$s-1\leq S\leq s+1. \tag{3.2}$$

Equations (3.1) and (3.2) do much to simplify the coupling schemes. The entire content of the model is summarized by a change of coupling transformation. Consider for example, isospin. The diquark and antidiquark with isospins i_1 and i_2, respectively, are coupled to total isospin I. The created quark-antiquark pair (each with $i=\frac{1}{2}$) are coupled to isospin zero. This isospin configuration may be expressed as a linear combination of Q^3 and $\bar{Q}^3$ states of good isospin as follows:

$$|(i_1i_2)^I(\tfrac{1}{2}\tfrac{1}{2})^0\rangle^I=\sum_{I_1I_2}\begin{bmatrix} i_1 & \frac{1}{2} & I_1\\ i_2 & \frac{1}{2} & I_2\\ I & 0 & I\end{bmatrix}|(i_1\tfrac{1}{2})^{I_1}(i_2\tfrac{1}{2})^{I_2}\rangle^I, \tag{3.3}$$

where I_1 (I_2) is the isospin of the baryon (antibaryon). The change of coupling coefficient is proportional to a 9-j symbol:

$$\begin{bmatrix} l_1 & s_1 & j_1\\ l_2 & s_2 & j_2\\ l_3 & s_3 & j_3\end{bmatrix}=[(2l_3+1)(2s_3+1)(2j_1+1)(2j_2+1)]^{1/2}\times\begin{Bmatrix} l_1 & s_1 & j_1\\ l_2 & s_2 & j_2\\ l_3 & s_3 & j_3\end{Bmatrix}. \tag{3.4}$$

All of the quantum numbers of the created $Q\bar{Q}$ pair must be coupled to the pre-existing $Q^2\bar{Q}^2$ state to determine the coupling to $B\bar{B}$ pairs. This includes spin, isospin, total angular momentum, and color. The result is

$$|(s_1i_1)(s_2i_2)slJI\rangle=\sum_{\substack{L=l\pm1,\,S\\(s_1I_1)(s_2I_2)}}C(l,L)\begin{bmatrix} s_1 & \frac{1}{2} & S_1\\ s_2 & \frac{1}{2} & S_2\\ s & 1 & S\end{bmatrix}\begin{bmatrix} i_1 & \frac{1}{2} & I_1\\ i_2 & \frac{1}{2} & I_2\\ I & 0 & I\end{bmatrix}\begin{bmatrix} s & l & J\\ 1 & 1 & 0\\ S & L & J\end{bmatrix}|(S_1I_1)(S_2I_2)SLJI\rangle. \tag{3.5}$$

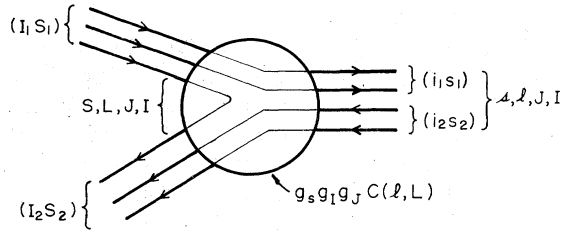

FIG. 4. Basic vertex of the $^3P_0$ model applied to the $B\bar{B}$ system. The three-point function is the product of known recoupling coefficients (g_s, g_I, and g_J) times an unknown factor $C(l,L)$.

A given $Q^2\bar{Q}^2$ state couples to various $B\bar{B}$ pairs, nucleons $(S_1I_1)=(\frac{1}{2},\frac{1}{2})$, and Δ's $(S_1I_1)=(\frac{3}{2},\frac{3}{2})$. The coefficient $C(l,L)$ is unknown. It is assumed to be independent of s, S, J, and I in the $^3P_0$ model. According to Eqs. (3.1) and (3.5) the $B\bar{B}$ couplings of all $Q^2\bar{Q}^2$ mesons with a given l value are known up to two constants, $C(l,l-1)$ and $C(l,l+1)$.

The color-recoupling coefficient is omitted from Eq. (3.5). It is the same for all states and therefore may be included in the unknown factor $C(l,L)$. Note that although Eq. (3.5) has the appearance of a change of coupling transformation, it is not unitary. Recouplings which result in colored baryons and antibaryons on the right-hand side have been omitted. Thus, for example, no $(S_1,I_1)=(\frac{3}{2},\frac{1}{2})$ baryon appears since it would, necessarily, be a color octet.

The coefficients which appear in Eq. (3.5) are tabulated in Tables V and VI. Table V lists spin and isospin coefficients only:

$$g_s \equiv \begin{bmatrix} s_1 & \frac{1}{2} & S_1 \\ s_2 & \frac{1}{2} & S_2 \\ s & 1 & S \end{bmatrix}, \tag{3.6}$$

$$g_I \equiv \begin{bmatrix} i_1 & \frac{1}{2} & I_1 \\ i_2 & \frac{1}{2} & I_2 \\ I & 0 & I \end{bmatrix}. \tag{3.7}$$

The product listed in columns of Table V includes a factor arising from the normalization of baryon wave functions. Thus, for example, the coupling of the $\delta\bar{\delta}$ state to $N\bar{N}$ is reduced by $\frac{1}{2}$ relative to $\Delta\bar{\Delta}$ and by $1/\sqrt{2}$ relative to $N\bar{\Delta}$ because the nucleon wave function consists of only 50% δ-type diquark, whereas the Δ consists entirely of δ-type diquark. Table VI lists the angular momentum recoupling factors:

$$g_J \equiv \begin{bmatrix} s & l & J \\ 1 & 1 & 0 \\ S & L & J \end{bmatrix}. \tag{3.8}$$

To obtain the coupling of a particular $Q^2\bar{Q}^2$ state to a specific $B\bar{B}$ channel it is necessary to combine the coefficients of Table V with those of Table VI. This is the subject of the following section, where the physics of specific channels will be discussed. Before leaving Tables V and VI it is worth noting several regularities. From Table V we note the following:

TABLE V. Spin and isospin coupling coefficients for $Q^2\bar{Q}^2$ coupling to $B\bar{B}$. g_s and g_I are defined by Eqs. (3.4) and (3.5), respectively. The column labeled "product" includes a factor of $1/\sqrt{2}$ for each nucleon in the $B\bar{B}$ state (see text).

State	$N\bar{N}$ coupling				$N\bar{\Delta}$ coupling				$\Delta\bar{\Delta}$ coupling			
(diquark content)$^{(I,s)}$	S	g_s	g_I	Product	S	g_s	g_I	Product	S	g_s	g_I	Product
A: $(\beta\bar{\beta})$	1	1	1	1/2								
B^+: $(1/\sqrt{2})(\beta\bar{\delta}+\delta\bar{\beta})$	1	$\sqrt{6}/3$	$\sqrt{3}/3$	1/3	1	$-\sqrt{3}/3$	$\sqrt{6}/3$	$-\sqrt{2}/6$				
					2	1	$\sqrt{6}/3$	$\sqrt{6}/6$				
B^-: $(1/\sqrt{2})(\beta\bar{\delta}-\delta\bar{\beta})$	0	-1	$\sqrt{3}/3$	$-\sqrt{6}/6$	1	$-\sqrt{3}/3$	$\sqrt{6}/3$	$-\sqrt{2}/6$				
					2	1	$\sqrt{6}/3$	$\sqrt{6}/6$				
C: $(\delta\bar{\delta})^{(0,0)}$	1	$-\sqrt{3}/9$	$\sqrt{3}/3$	$-1/18$					1	$\sqrt{30}/9$	$\sqrt{6}/3$	$2\sqrt{5}/9$
C: $(\delta\bar{\delta})^{(1,0)}$	1	$-\sqrt{3}/9$	$\sqrt{2}/3$	$-\sqrt{6}/54$	1	$2\sqrt{6}/9$	$-1/3$	$-2\sqrt{3}/27$	1	$\sqrt{30}/9$	$\sqrt{5}/3$	$2\sqrt{6}/27$
C: $(\delta\bar{\delta})^{(2,0)}$					1	$2\sqrt{6}/9$	$-\sqrt{3}/3$	$-2/9$	1	$\sqrt{30}/9$	$\sqrt{3}/3$	$\sqrt{10}/9$
C: $(\delta\bar{\delta})^{(0,1)}$	0	$\sqrt{6}/3$	$\sqrt{3}/3$	$\sqrt{2}/6$					1	$-\sqrt{3}/3$	$\sqrt{6}/3$	$-\sqrt{2}/3$
									2	$\sqrt{6}/3$	$\sqrt{6}/3$	$2/3$
C: $(\delta\bar{\delta})^{(1,1)}$	0	$\sqrt{6}/3$	$\sqrt{2}/3$	$\sqrt{3}/9$	1	$\sqrt{2}/2$	$-1/3$	$-1/6$	0	$-\sqrt{3}/3$	$\sqrt{5}/3$	$-\sqrt{15}/9$
					2	$\sqrt{6}/6$	$-1/3$	$-\sqrt{3}/18$	2	$\sqrt{6}/3$	$\sqrt{5}/3$	$\sqrt{30}/9$
C: $(\delta\bar{\delta})^{(2,1)}$					1	$\sqrt{2}/2$	$-\sqrt{3}/3$	$-\sqrt{3}/6$	0	$-\sqrt{3}/3$	$\sqrt{3}/3$	$-1/3$
					2	$\sqrt{6}/6$	$-\sqrt{3}/3$	$-1/6$	2	$\sqrt{6}/3$	$\sqrt{3}/3$	$\sqrt{2}/3$
C: $(\delta\bar{\delta})^{(0,2)}$	1	$2\sqrt{15}/9$	$\sqrt{3}/3$	$\sqrt{5}/9$					1	$-\sqrt{6}/9$	$\sqrt{6}/3$	$-2/9$
									3	1	$\sqrt{6}/3$	$\sqrt{6}/3$
C: $(\delta\bar{\delta})^{(1,2)}$	2	$2\sqrt{15}/9$	$\sqrt{2}/3$	$\sqrt{30}/27$	1	$\sqrt{30}/18$	$-1/3$	$-\sqrt{15}/54$	1	$-\sqrt{6}/9$	$\sqrt{5}/3$	$-\sqrt{10}/9$
					2	3/4	$-1/3$		3	1	$\sqrt{5}/3$	$\sqrt{5}/3$
C: $(\delta\bar{\delta})^{(2,2)}$					1	$\sqrt{30}/18$	$-\sqrt{3}/3$	$-\sqrt{5}/54$	1	$-\sqrt{6}/9$	$\sqrt{3}/3$	$-\sqrt{2}/9$
					2	3/4	$-\sqrt{3}/3$	$-\sqrt{6}/8$	3	1	$\sqrt{3}/3$	$\sqrt{3}/3$

TABLE VI. The angular momentum recoupling factor, defined by Eq. (3.6) for coupling $Q^2\bar{Q}^2$ states to $N\bar{N}$. Note $N\bar{\Delta}$ or $\Delta\bar{\Delta}$ couplings would require additional calculation.

States (diquark content)	$\mathcal{S}$	J	S	L	g_J^2
$\beta\bar{\beta}$	0	l	1	$l-1$	$\frac{2l-1}{3(2l+1)}$
		l	1	$l+1$	$\frac{2l+3}{3(2l+1)}$
$\frac{1}{\sqrt{2}}(\beta\bar{\delta}+\delta\bar{\beta})$	1	$l-1$	1	$l-1$	$\frac{l-1}{6l}$
		l	1	$l-1$	$\frac{(2l-1)(l+1)}{6l(2l+1)}$
		l	1	$l+1$	$\frac{l(2l+3)}{6(l+1)(2l+1)}$
		$l+1$	1	$l+1$	$\frac{l+2}{6(l+1)}$
$\frac{1}{\sqrt{2}}(\beta\bar{\delta}-\delta\bar{\beta})$	1	$l-1$	0	$l-1$	$\frac{1}{3}$
		$l+1$	0	$l+1$	$\frac{1}{3}$
$\delta\bar{\delta}$	0	l	1	$l-1$	$\frac{2l-1}{3(2l+1)}$
		l	1	$l+1$	$\frac{2l+3}{3(2l+1)}$
$\delta\bar{\delta}$	1	$l-1$	0	$l-1$	$\frac{1}{3}$
		$l+1$	0	$l+1$	$\frac{1}{3}$
$\delta\bar{\delta}$	2	$l-2$	1	$l-1$	$\frac{1}{5}$
		$l-1$	1	$l-1$	$\frac{l+1}{10l}$ [a]
		l	1	$l-1$	$\frac{(l+1)(2l+3)}{30(2l+1)}$
		l	1	$l+1$	$\frac{l(2l-1)}{30(l+1)(2l+1)}$
		$l+1$	1	$l+1$	$\frac{l}{10(l+1)}$
		$l+2$	1	$l+1$	$\frac{1}{5}$

[a] Zero for $l=1$.

(1) The $\mathcal{S}=0$ $\delta\bar{\delta}$ state is relatively very weakly coupled to $N\bar{N}$.

(2) $\beta\bar{\beta}$ and $\beta\bar{\delta}\pm\delta\bar{\beta}$ dominate the $N\bar{N}$ couplings.

From Table VI we note the following:

(1) States with higher $\mathcal{S}$ are more weakly coupled especially when $\mathcal{S}$ is coupled to l to yield $J\approx l$. These regularities will simplify the spectroscopy outlined in the following section.

The final ingredient we employ in determining $B\bar{B}$ couplings to $Q^2\bar{Q}^2$ is peripherality,[4] by which we mean the qualitative observation that resonance formation in two-body channels occurs at a fixed impact parameter independent of center-of-mass energy. This idea was first introduced in the $B\bar{B}$ system motivated by the observation that small-impact-parameter interactions are dominated by annihilation and large impact parameters are outside the range of the force. This leaves a ring of fixed radius for resonance formation. Subsequently peripherality became a central ingredient in the notion of two-component duality.[9] Quantitatively peripherality amounts to the observation that prominant resonances follow the curve $L\approx kR$, where R is a fixed radius characteristic of the specific channel and k is the center-of-mass momentum. In the $B\bar{B}$ system, Carter *et al.*[20] have found a series of resonances which appear to fall on a curve $L\approx kR$ with $R\approx 1/m_\pi$. For our estimates we will take 1.3 fm $< R <$ 1.5 fm. It should be emphasized that we use this notion only qualitatively. We do not try to discriminate subtle differences among states relatively close to the peripherality curve. On the other hand we *do* assume that states, say, two units in L distant from the peripheral curve will be suppressed.

IV. APPLICATIONS

In this section we bring together the results of earlier calculations and apply them to some familiar baryon-antibaryon processes. It should be stressed that these examples are only illustrative. The content of this paper lies in the tables of trajectories and coupling constants (Tables III, V, and VI). The reader may construct the model's predictions for the channel of his choice by combining those results consistently with the dynamics outlined in Sec. III. To facilitate this we present now a brief directory to the information contained in the paper and a summary of the dynamical rules we have proposed:

(1) Masses and quantum numbers of $Q^2\bar{Q}^2$ states: Table III (in a diquark-antidiquark basis).

(2) Couplings to $B\bar{B}$ channels: Table V (spin and isospin factors), Table VI (angular momentum factors).

(3) Selection rules and other dynamics:

(A) $\mathcal{S}=S$, $S+1$, or $S-1$ only ($^3P_0$ model).

(B) $L=l\pm 1$ only ($^3P_0$ model plus parity).

(C) Coupling coefficients of Tables V and VI are only valid when comparing systems with the same l and L.

(D) Peripherality: $Q^2\bar{Q}^2$ resonances lying closest to the curve $L=kR$ are expected to most strong-

TABLE VII. Relative strengths of $N\bar{N}$ couplings to $L=l+1$ $Q^2\bar{Q}^2$ trajectories are listed. For each l value the relative couplings of trajectories may be compared. Different l values are not related. All C-type trajectories have (degenerate) $I=0$ and 1 members. The $I=0$ coefficient is listed, the $I=1$ coefficient is smaller by a factor $\frac{2}{3}$.

	1	2	3	4	5		6		7
	$A(J=l)$	$B^+(J=l)$	$B^+(J=l+1)$	$B^-(J=l+1)$	$C(J=l)$		$C(J=l+1)$		$C(J=l+2)$
l	$I=0$	$I=1$	$I=1$	$I=1$ $I=0$	$S=0$	$S=2$	$S=1$	$S=2$	$I=0$
1	0.14	0.010	0.028	0.019	0.0017	0.000 34	0.0062	0.0031	0.012
2	0.12	0.017	0.025	0.019	0.0015	0.000 82	0.0062	0.0041	0.012
3	0.11	0.018	0.023	0.019	0.0013	0.001 1	0.0062	0.0046	0.012
4	0.10	0.018	0.022	0.019	0.0013	0.001 3	0.0062	0.0049	0.012
5	0.10	0.018	0.022	0.019	0.0012	0.001 4	0.0062	0.0051	0.012
∞	0.083	0.019	0.019	0.019	0.0010	0.002 1	0.0062	0.0062	0.012

ly excited; states far from this curve are expected to be very difficult to observe. For purposes of estimation we take $R\cong 1/m_\pi$, specifically, 1.3 fm $< R <$ 1.5 fm. With these in mind we proceed to look at the following $B\bar{B}$ systems:

(A) Elastic $N\bar{N}$ scattering,

(B) $N\bar{N}\to\pi^+\pi^-$ (with remarks about $\pi^0\pi^0$, $\pi^0\eta$, etc.),

(C) $Q^2\bar{Q}^2$ states at or below $N\bar{N}$ threshold,

(D) exotics in the $B\bar{B}$ system.

A. Elastic $N\bar{N}$ scattering

Figures 5–8 are Chew-Frautschi diagrams of $Q^2\bar{Q}^2$ trajectories coupling to elastic $N\bar{N}$ scattering. The spin-singlet ($J=L$) and spin-triplet ($J=L-1$, L, and $L+1$) channels are displayed separately. The peripherality band ($L=kR$ with $R=1.3$–1.5 fm) is superimposed on each graph. The quark content of trajectories is labeled with the shorthand notation from Table II:

$$A=\beta\bar{\beta},$$
$$B^\pm=(\beta\bar{\delta}\pm\delta\bar{\beta})/\sqrt{2}, \qquad (4.1)$$
$$C=\delta\bar{\delta}.$$

The quark spin (S) and isospin (I) are labeled on each trajectory.

For a given value of l, the relative couplings to $N\bar{N}$ of all trajectories with $L=l+1$ are fixed by the coupling constants of Table V and VI. (The spin-isospin factor of Table V is to be multiplied by the angular momentum factor from Table VI. The elastic $N\bar{N}$ coupling is proportional to the square of this number.) Table VII lists the relative couplings for the case $L=l+1$. The same analysis applies to $L=l-1$. The resulting relative couplings are listed in Table VIII. Clearly some trajectories are highly suppressed. To be systematic we consider each channel in turn.

$J=L-1$ (Fig. 5): This channel contains the most prominent resonances. From Table VII columns 1, 2, and 5 we see that the $A(J=l)$, $B^+(J=l)$, and $C(J=l)$ trajectories are coupled in roughly the ratios 6:1:$\frac{1}{15}$. The $C(J=l-2)$ trajectory cannot be compared because it belongs to the $L=l-1$ family. The trajectories $A(J=l)$ and $B^+(J=l)$ are quite close to the peripherality curve. The $C(J=l-2)$ trajectory is far from the peripherality curve and its couplings are therefore suppressed. *We conclude that a relatively strong isospin-0 $[A(J=l)]$ trajectory is expected, accompanied by a substantially weaker (by a factor of 5 for $l\gtrsim 3$) isospin-1*

TABLE VIII. Relative strengths of $N\bar{N}$ couplings to $L=l-1$ $Q^2\bar{Q}^2$ trajectories are listed. For each l value the relative couplings of trajectories may be compared. Different l values are not related. All C-type trajectories have (degenerate) $I=0$ and 1 members. The $I=0$ coefficient is listed, the $I=1$ coefficient is smaller by a factor $\frac{2}{3}$.

					$C(J=l)$		$C(J=l-1)$		
	$A(J=l)$	$B^+(J=l)$	$B^+(J=l-1)$	$B^-(J=l-1)$	$S=0$	$S=2$	$S=1$	$S=2$	$C(J=l-2)$
	$I=0$	$I=1$	$I=1$	$I=1$	$I=0$		$I=0$		$I=0$
1	0.028	0.012	0	0.019	0.000 34	0.0069	0.0062	0	0.012
2	0.050	0.017	0.0093	0.019	0.000 62	0.0043	0.0062	0.0093	0.012
3	0.060	0.018	0.012	0.019	0.000 73	0.0035	0.0062	0.0082	0.012
4	0.065	0.018	0.014	0.019	0.000 80	0.0031	0.0062	0.0077	0.012
5	0.068	0.018	0.015	0.019	0.000 84	0.0029	0.0062	0.0074	0.012
∞	0.083	0.019	0.019	0.019	0.001 0	0.0021	0.0062	0.0062	0.012

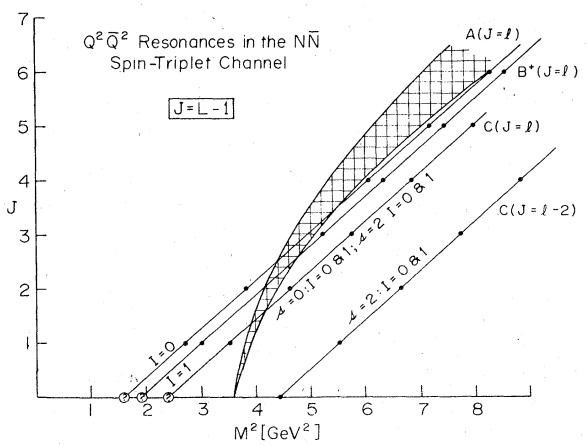

FIG. 5. $Q^2\bar{Q}^2$ trajectories which couple to the spin-triplet $N\bar{N}$ system with $J=L-1$. Trajectories are labeled in the notation of Tables II and III. $Q^2\bar{Q}^2$ states with $l=0$ which are expected to mix strongly and not couple strongly to $N\bar{N}$ are denoted by (?). The peripherality curve: $L=kR$ for 1.3 fm $< R <$ 1.5 fm is shown hatched.

trajectory. None of the C-type trajectories will be seen.

$J=L+1$ (Fig. 6): Little resonant structure is to be expected in this channel. Only the $C(J=l+2)$ trajectory lies close enough to the peripherality curve to be important. Notice that no trajectory in Fig. 6 is as peripheral as the A and B^+ trajectories in Fig. 5. The couplings of $C(J=l+2)$ states to $N\bar{N}$ can be compared with other $L=l+1$ trajectories, in particular with the prominent states in Fig. 5. From column 7 of Table VII we see that it couples 7 to 10 times less strongly than the $A(J=l)$ trajectory in $J=L+1$.

$J=L$ spin triplet (Fig. 7): The trajectories $B^+(J=l+1)$ and $C(J=l+1)$ are perhaps close enough

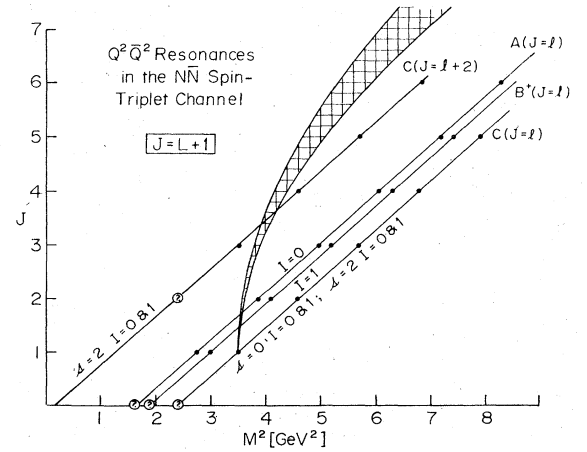

FIG. 6. $Q^2\bar{Q}^2$ trajectories which couple to the spin-triplet $N\bar{N}$ system with $J=L+1$. Other details as in Fig. 5.

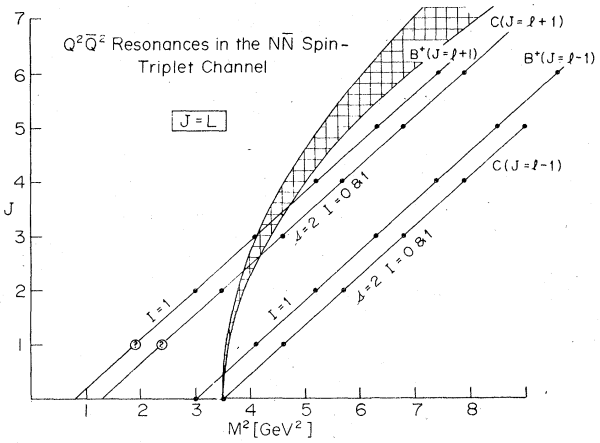

FIG. 7. $Q^2\bar{Q}^2$ trajectories which couple to the spin-triplet $N\bar{N}$ system with $J=L$. Other details as in Fig. 5.

to the peripherality line to be prominent. According to Table VII the C-type state (column 6) is weakly coupled—roughly $\frac{1}{40}$ to $\frac{1}{12}$ the leading $A(J=l)$ trajectory. The $B^+(J=l+1)$ trajectory is, on the other hand, rather strongly coupled—roughly $\frac{1}{5}$ to $\frac{1}{4}$ the leading $A(J=l)$ trajectory. We expect a fairly strong isospin-1 trajectory and a weak $I=0$ and 1 pair of trajectories in this channel.

$J=L$ spin singlet (Fig. 8): The trajectories $B^-(J=l+1)$ and $C(J=l+1)$ are perhaps close enough to the peripherality line to be prominent. The $B^-(J=l+1)$ trajectory is more strongly coupled [roughly $\frac{1}{8}$ to $\frac{1}{4}$ the leading $A(J=l)$ trajectory], the $C(J=l+1)$ trajectory is down by a factor of 3. Again we expect a fairly strong isospin-1 trajectory but also may find a less prominent $I=0$ and 1 pair of trajectories.

Note that peripherality has excluded all trajectories in Table VIII, i.e., those with $L=l-1$. This is an important result. For some trajectories

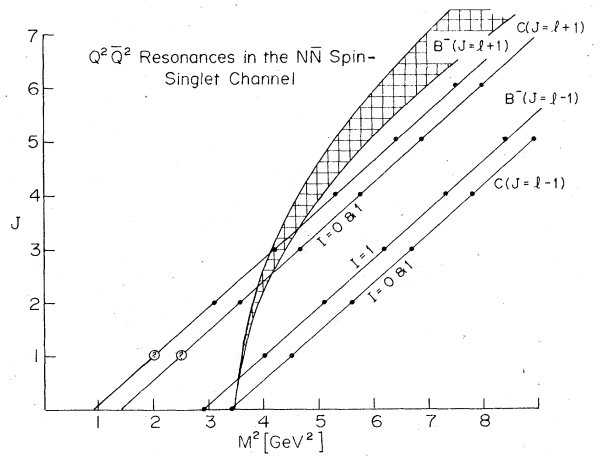

FIG. 8. $Q^2\bar{Q}^2$ trajectories which couple to the spin-singlet $N\bar{N}$ system ($J=L$). Other details as in Fig. 5.

TABLE IX. Masses and spin-parities of most prominent $Q^2\bar{Q}^2$ resonances in elastic $N\bar{N}$ scattering. Couplings are given qualitatively. See text and Table VII for more complete information. Masses are in GeV.

Channel	$J=L-1$				Triplet $J=L$		Singlet $J=1$				$J=L+1$	
Trajectory	$A(J=l)$		$B^+(J=l)$		$B^+(J=l+1)$		$B^-(J=l+1)$		$C(J=l+1)$		$C(J=l+2)$	
$N\bar{N}$ coupling	Strong		Moderate		Moderate		Moderate		Weak		Weak	
Isospin	0		1		1		1		0, 1		0, 1	
l	J^P	M	J^P	M	J^P	M	J^P	M	J^P	M	J^P	M
1	1^-	1.65	1^-	1.73	2^-	1.73	2^-	1.73	2^-	1.87	3^-	1.87
2	2^+	1.96	2^+	2.02	3^+	2.02	3^+	2.02	3^+	2.15	4^+	2.15
3	3^-	2.22	3^-	2.28	4^-	2.28	4^-	2.28	4^-	2.39	5^-	2.39
4	4^+	2.46	4^+	2.51	5^+	2.51	5^+	2.51	5^+	2.62	6^+	2.62
5	5^-	2.67	5^-	2.73	6^-	2.73	6^-	2.73	6^-	2.82	7^-	2.82
6	6^+	2.87	6^+	2.92	7^+	2.92	7^+	2.92	7^+	3.01	8^+	3.01
7	7^-	3.06	7^-	3.11	8^-	3.11	8^-	3.11	8^-	3.19	9^-	3.19

(those with $J=l$) it implies that they couple predominantly only to one $N\bar{N}$ partial wave ($J=L-1$). For others, (e.g. all trajectories with $J<l-1$) it implies they will be difficult to see at all in $N\bar{N}$. This is the $Q^2\bar{Q}^2$ analog of a well-known effect among the $Q\bar{Q}$ mesons: In $\pi\pi$ scattering the scalar trajectory (in the quark model $J=L=l-1$) is suppressed relative to the tensor trajectory ($J=L=l+1$ in the quark model) because it lies so far below the curve $L=kR$.

All possibly prominent trajectories came from Table VII. For each value of l their couplings are determined up to one overall constant. To summarize our findings we have listed the most prominent states in Table IX with both masses and couplings.

Even though most $Q^2\bar{Q}^2$ trajectories have been eliminated from consideration, our quark model is still too crude to enable us to unambiguously classify known elastic $N\bar{N}$ resonances as specific $Q^2\bar{Q}^2$ states. From Table IX we expect a strong isosinglet and three moderate isotriplet resonances in the regions of 1.99, 2.25, 2.49, 2.70 GeV, etc. Perhaps these are to be identified with the known S, T, and U resonances (Table X). Errors of even hundreds of MeV in the mass scale are not surprising considering the manner in which intercepts are calculated in our model. The differences in spacing is more disturbing. We will discuss it more fully in the context of $N\bar{N}\to\pi\pi$. In any event as Table IX illustrates, even the low-energy resonant structure in $N\bar{N}$ is likely to be quite complex, with many overlapping, interfering resonances.

TABLE X. Resonances observed in elastic $N\bar{N}$ scattering.

	I	Mass (MeV)	Width (MeV)
S	1 (0)	1932 ± 2	9^{+4}_{-3}
T	1	2190 ± 10	90 ± 20
U	1	2350 ± 10	160 ± 20
	0	2375 ± 10	190 ± 20

B. $N\bar{N}\to\pi^+\pi^-$

The reaction $N\bar{N}\to\pi^+\pi^-$ has two attractive features from our standpoint: First, only the initial states $J=L\pm1$ are allowed (parity); second, $G=+1$ eliminates every other state on any given trajectory of fixed isospin. The couplings of $N\bar{N}$ to $\pi\pi$ are products of the square roots of the coefficients in Tables VII and VIII times couplings for a $Q^2\bar{Q}^2$ state to go to $\pi\pi$, about which we know little. Relying on our knowledge of $N\bar{N}$ couplings alone, we exclude the $J=L+1$ channel here as we did above in $N\bar{N}$ elastic scattering. The remaining trajectories, coupling to the $J=L-1$ $N\bar{N}$ channel are shown in Fig. 9. As in the analysis of $N\bar{N}$ elastic scattering only the $A(J=l)$ and $B^+(J=l)$ trajectories are expected to couple strongly. We are led to predict the following resonances:

$J^{PC}I^G=2^{++}0^+$, $M=1.96$ GeV

$J^{PC}I^G=3^{--}1^+$, $M=2.28$ GeV

$J^{PC}I^G=4^{++}0^+$, $M=2.46$ GeV

$J^{PC}I^G=5^{--}1^+$, $M=2.73$ GeV

$J^{PC}I^G=6^{++}0^+$, $M=2.87$ GeV.

Recently Carter *et al.*[20] have completed an amplitude analysis of this process in which they find evidence for resonances as follows:

$J^{PC}I^G=3^{--}1^+$ $M=2.15$ GeV $\Gamma=200$ MeV,

$J^{PC}I^G=4^{++}0^+$ $M=2.31$ GeV $\Gamma=210$ MeV,

$J^{PC}I^G=5^{--}1^+$ $M=2.48$ GeV $\Gamma=280$ MeV.

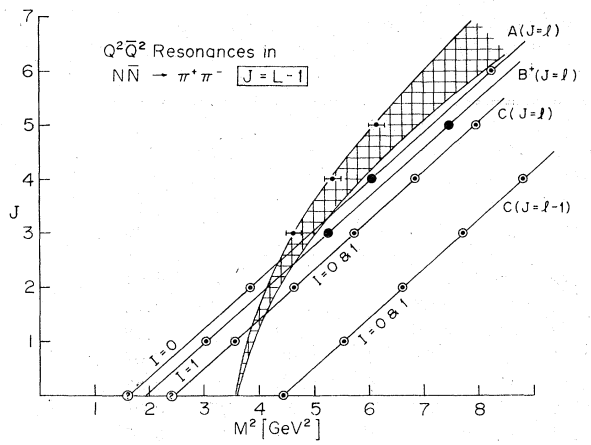

FIG. 9. Q^2Q^2 trajectories which couple both to $N\bar{N}$ and $\pi^+\pi^-$ in the $J=L-1$ channel of $N\bar{N}$. Expected states are marked by circled points. States of Carter *et al.* (Ref. 20) are shown with error bars. Candidate $Q^2\bar{Q}^2$ states are marked by solid circles. Other details as in Fig. 5.

These states are rather wide but their branching ratios into $\pi^+\pi^-$ are quite small (of order 1%). This is consistent with (but does not require) their being predominantly elastic $N\bar{N}$ resonances such as we have described. Furthermore Carter *et al* find that their resonances couple 2 to 3 times more strongly (*in amplitude*) to the $J=L-1$ partial wave than to the $J=L+1$ partial wave.

The agreement with our expectations is about as good as can be expected in light of the crudeness of our model. Since the overall mass scale of the $Q^2\bar{Q}^2$ trajectories is not tied to the $B\bar{B}$ system (except insofar as the bag constant, $B^{1/4}=146$ MeV, was fit in an analysis which included the nucleon), it is nontrivial that the absolute mass scale is off only by 5 or 10%. Looking at Fig. 9, one might be tempted to use the masses of the three resonances to fix the intercepts of the $A(J=l)$ and $B^+(J=1)$ trajectories. We leave this sort of analysis to the day when both theory and experiment are more well defined.

As Fig. 9 shows, the resonances of Carter *et al.* appear to follow the peripherality curve or a straight-line Regge trajectory with greater than usual slope. Assuming the former to be the case it would be tempting to seek an optical interpretation of the resonances outside the quark model.[21] The prominent resonances might be expected to lie on the intersection of the $N\bar{N}$ and $\pi\pi$ peripherality curves: $L=k(N\bar{N})R_{N\bar{N}}$ and $L_{\pi\pi}(=J)=k(\pi\pi)R_{\pi\pi}$, where $L_{\pi\pi}$, $k(\pi\pi)$, and $R_{\pi\pi}$ are the orbital angular momentum, center-of-mass momentum, and interaction radius, respectively, in the $\pi\pi$ system. This predicts that the low-spin ($J\approx 3$) resonances appear in the $J=L+1$ channel and high-spin resonances ($J\approx 5$) in the $J=L-1$ channel, contrary to the data. If $B\bar{B}$ resonances do indeed lie on Regge trajectories of high slope, the implication would be disturbing: Either (some) $Q^2\bar{Q}^2$ trajectories have greater slopes than $Q\bar{Q}$ trajectories (and will be the leading trajectories at high mass), or curvature persists to high l in the $Q^2\bar{Q}^2$ sector, or the three resonances lie on three different ordinary $Q^2\bar{Q}^2$ trajectories and the appearance of a higher slope is accidental.

Other mesonic final states are also good filters through which to study the $B\bar{B}$ system. $\pi^0\pi^0$ selects $J=L\pm1$ and only J even, $I=0$. The prominent states can be read off Fig. 9. $\pi^0\eta^0$ selects $J=L\pm1$, $I=1$, and odd G parity. Once again the prominent states can be read off Fig. 9. Final states involving vector mesons ($\pi\rho$ and $\pi\omega$, for example) can be produced in either the $J=L$ or $J=L\pm1$ $N\bar{N}$ channels. With many overlapping resonances these processes will not be easy to sort out. A scalar-pseudoscalar final state would select the otherwise difficult to see $J=L$ (spin singlet and triplet) $N\bar{N}$ channels. Information on $N\bar{N}\to\pi S^*$ (via $N\bar{N}\to\pi K\bar{K}$) and $N\bar{N}\to\pi\delta$ (via $N\bar{N}\to\pi\pi\eta$) would be as useful as it would be difficult to obtain.

C. $Q^2\bar{Q}^2$ States at or below $N\bar{N}$ threshold

Figures 5–8 show many $Q^2\bar{Q}^2$ states coupling to $N\bar{N}$ near threshold. Most are not likely to be prominent for several reasons. First $l=0$ $Q^2\bar{Q}^2$ states are primarily meson-meson states. They are likely to be broad if resonant at all, and only weakly coupled to $N\bar{N}$. Of the $l=1$ states, several are $J^{PC}=0^{--}$ states which decoupled from $N\bar{N}$. We are left with a family of $l=1$ $Q^2\bar{Q}^2$ states with masses between 1.65 and 1.87 GeV. These are listed in Table XI. All $l=2$ states are well above threshold.

So all candidates for $N\bar{N}$ states near threshold in our model have $l=1$. *They must have negative parity*. Unfortunately, the model is worse for low l than for high l as we have repeatedly emphasized. Trajectories are expected to show curvature at low l. This introduces uncertainties into our mass estimates. In addition, our argument against purely mesonic decays requires large l. States as low as $l=1$ may be expected to have rather large widths into meson final states.

The experimental situation regarding $N\bar{N}$ states near threshold has been reviewed by Kalogeropoulos.[22] The best candidate for such a state is an $I^G=1^+$ enhancement observed by Gray *et al.*[23] at 1795 MeV with a <15 MeV width. Other enhancements nearer threshold have been reported,[22] but all of these states are in need of confirmation.

TABLE XI. Quantum numbers, masses, and couplings to $N\bar{N}$ of $Q^2\bar{Q}^2$ states predicted to be at or below threshold. The strength of the $A(J=l)$ coupling to $N\bar{N}$ is normalized to unity in both the $L=0$ and 2 partial waves.

State	$J^{PC}I^G$	L	Mass (GeV)	Relative coupling to $N\bar{N}$ $L=l-1$	$L=l+1$
$A(J=l)$	$1^{--}0^-$	0, 2	1.65	1	1
$B^+(J=l)$	$1^{--}1^+$	0, 2	1.73	0.44	0.07
$B^+(J=l+1)$	$2^{--}1^+$	2	1.73	···	0.20
$B^-(J=l-1)$	$0^{-+}1^-$	0	1.73	0.69	···
$B^-(J=l+1)$	$2^{-+}1^-$	2	1.73	···	0.14
$C(J=l-1)$ $S=1$	$0^{-+}0^+$	0	1.87	0.23	···
	$0^{-+}1^-$	0	1.87	0.15	···
$C(J=l)$ $S=2$	$1^{--}0^-$	0, 2	1.87	0.25	2.4×10^{-3}
	$1^{--}1^+$	0, 2	1.87	0.17	1.6×10^{-3}
$C(J=l)$ $S=0$	$1^{--}0^-$	0, 2	1.87	1.2×10^{-2}	1.2×10^{-2}
	$1^{--}1^+$	0, 2	1.87	8.3×10^{-3}	8.1×10^{-3}
$C(J=l+1)$ $S=1$	$2^{-+}0^+$	2	1.87	···	4.4×10^{-2}
	$2^{-+}1^-$	2	1.87	···	3.0×10^{-2}
$C(J=l+1)$ $S=2$	$2^{--}0^-$	2	1.87	···	2.2×10^{-2}
	$2^{--}1^+$	2	1.87	···	1.1×10^{-2}
$C(J=l+2)$ $S=2$	$3^{--}0^-$	2	1.87	···	8.6×10^{-2}
	$3^{--}1^+$	2	1.87	···	5.7×10^{-2}

Only the $I=1$ channel $(\bar{p}+d\to(N\pi)+p)$ has been studied. An analogous study of $I=0$ would require the identification of a neutron spectator.

Naively one would expect annihilation at rest to be dominated by the S wave. If so we can identify two candidates for the 1795 MeV state: The $B^+(J=l)$ state predicted to be at 1730 MeV, or the $C(J=l)$ $S=2$ state predicted at 1870 MeV.[24] Either assignment suffers from an important problem; an $I^G=1^-$ state lies roughly degenerate with the $I^G=1^+$ candidate. The experiment of Gray *et al.* should have been sensitive to odd-pion final states, but detected no enhancement. If either of these assignments is correct the $I^G=1^-$ state would have to be weakly coupled for reasons unexplained in our model.

Perhaps, as has been suggested, S-wave $N\bar{N}$ resonances near threshold are very broad. One would then look for candidates among the pure D-wave states of Table X. Unfortunately, the same problem arises: Each $I^G=1^+$ state is accompanied by a roughly degenerate $I^G=1^-$ brother. The only hope we can offer the experimentalist is the anticipation of a long and fruitful career discovering and classifying $N\bar{N}$ states at and below threshold.

D. $I=2$ $Q^2\bar{Q}^2$ Resonances which couple to $B\bar{B}$

All $I=2$ $Q^2\bar{Q}^2$ resonances which couple to $B\bar{B}$ arise from the $\delta\bar{\delta}$ configuration which may couple to quark spin $S=0$, 1 or 2. There are therefore a large number of exotic isotensor trajectories for each value of l with total angular momentum ranging from $J=|l-2|$ to $J=l+2$. The last of these is the leading trajectory. In the $N\bar{N}$ system the isoscalar and isovector analogs of this trajectory are likely not to be prominent because they couple only to the $J=L+1$ channel and therefore fall below the peripherality curve [see the $C(J=l+2)$ trajectory in Fig. 6]. The $N\bar{\Delta}$ and $\Delta\bar{\Delta}$ thresholds are higher and the associated peripherality curves are lower (see Fig. 10). Consequently high-J states on the $C(J=l+2)$ trajectory are likely to be prominent in $N\bar{\Delta}$ and $\Delta\bar{\Delta}$ channels.

The analysis we performed for the $N\bar{N}$ elastic scattering could be repeated for the $N\bar{\Delta}$ and $\Delta\bar{\Delta}$ isotensor states. This is an extensive undertaking and probably not warranted by the present state

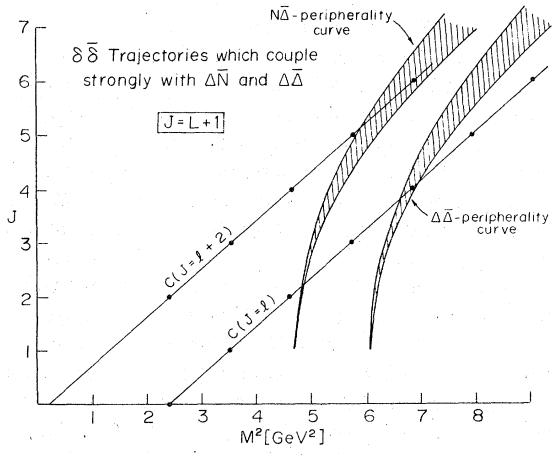

FIG. 10. Peripherality curves for $N\bar{\Delta}$ and $\Delta\bar{\Delta}$ systems are shown along with two (strongly coupled) $\delta\bar{\delta}$ trajectories in the $J=L+1$ channel.

of data on exotics in $B\bar{B}$ channels. Instead we will list the masses of these groups of states (taken from Table II) and for each l (and therefore each mass) we list the dominant partial wave (L value) in the $N\bar{\Delta}$ system estimated from the peripherality curve. The results are listed in Table XII. The $l=2$ states near the $N\bar{\Delta}$ threshold do not couple to the $N\bar{\Delta}$ S-wave and may therefore be suppressed. The 2.62-GeV states are tantalizingly close to the possible controversial isotensor state at 2.67 GeV reported by Rogers at the 1977 Experimental Meson Spectroscopy Conference.[25] Unfortunately there are many possible $N\bar{\Delta}$ states in the group at 2.62 GeV, a $J^P=4^+$ state (from $S=0$), $J^P=3^+, 4^+, 5^+$ (from $S=1$), and $J^P=3^+, 4^+, 5^+$, 6^+ (from $S=2$), so no more specific assignment is possible. Clearly more theoretical input is necessary to establish which states are prominent and which are suppressed.

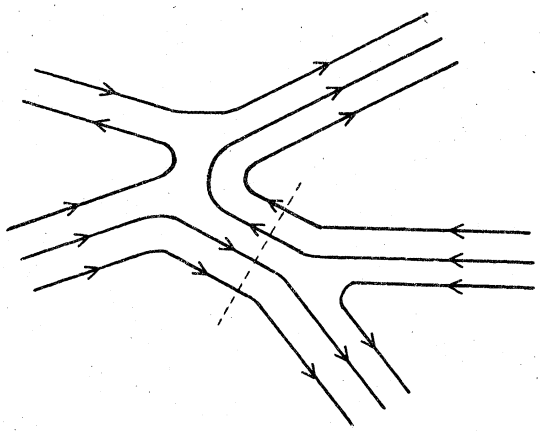

FIG. 11. Harari-Rosner diagram for $\pi N \to N_f(N\bar{N})$ showing antibaryon exchange and $Q^2\bar{Q}^2$ resonance production.

V. DISCUSSION AND CONCLUSION

In the $B\bar{B}$ system nature has provided us with a means to study an entire sector of the quark spectrum which would otherwise remain largely unknown. It should provide many tests of quark-model ideas developed in the study of more conventional meson and baryon spectroscopy. We have mentioned several. Foremost is the classification scheme of $SU(3)_{color} \times SU(3)_{flavor} \times SU(2)_{spin}$. Perhaps most interesting is the added importance of color in the $Q^2\bar{Q}^2$ sector: Several families of trajectories differing in color content should exist, but only one ($\bar{3}$-3) should couple strongly to $B\bar{B}$. Also color "configuration mixing" appears to be a potential source of curvature in Regge trajectories at low J. The $^3P_0$ model can be tested extensively once sets of resonances have been identified and classified. Of particular interest is the selection rule $L=l\pm1$, which has not been tested in ordinary baryon and meson decays. Also of great interest are the universality of the Regge slope (for $\bar{3}$-3 trajectories); the absence of strong $\vec{l}\cdot\vec{S}$ coupling in the quark model and the possibility of observing, for the first time, unambiguous exotic states.

This paper is admittedly rudimentary. We have only imitated in the $Q^2\bar{Q}^2$ sector what was done many years ago in the $Q\bar{Q}$ sector. There are several important questions which our methods have been unable to address. First we are unable to estimate absolute widths. A most surprising feature of the $B\bar{B}$ resonances discovered in recent years is the variation in their widths,[1] which range from $\lesssim 8$ to 280 MeV. Second, we have not discussed production experiments such as $\pi^- p \to p_f(p\bar{p}\pi^-)$ in which prominent, narrow resonances are known.[23] These are typically interpreted in terms of antibaryon exchange as shown in Fig. 11. Our model for couplings is limited to on-shell $B\bar{B}$ initial states. One interesting speculation regarding production experiments involves the 6-$\bar{6}$-type $Q^2\bar{Q}^2$ trajectories which we discarded early in Sec. II. These states couple weakly both to $B\bar{B}$ and to mesons. They are candidates for very narrow $Q^2\bar{Q}^2$ states, but are also difficult to form in $B\bar{B}$ elastic scattering. If, for some as yet unknown reason, they were more strongly coupled to production processes they might be candidates for the narrow states recently reported.[23] An essential test of this idea would be an anomalously small $\alpha' = 0.57\ \mathrm{GeV}^{-2}$ Regge slope.

If the quark-model classification scheme (which works so well for $Q\bar{Q}$ and Q^3 states) also applies in the $Q^2\bar{Q}^2$ sector, then hundreds of $B\bar{B}$ resonances in the region between 1.6 and 3.0 GeV await discovery. The spectrum is rich but not beyond sorting out. Any new dynamical ideas developed from quantum chromodynamics should immediately be pressed into service to this end.

TABLE XII. Masses of $Q^2\bar{Q}^2$ isotensor resonances.

l	Mass (GeV)	Dominant Partial Wave in $N\bar{\Delta}$ (L)
1	1.87	*
2	2.15	1
3	2.39	4
4	2.62	5
5	2.82	6
6	3.01	7

ACKNOWLEDGMENTS

Elements of this work were inspired by conversations with T. Kalogeropoulos and J. Rosner. In addition, helpful suggestions and conversations from K. Johnson, J. Rosner, and C. B. Thorn are gratefully acknowledged. The generous hospitality of Nordita, where this work was begun, and the Aspen Center for Physics, where it was completed, were most appreciated. This work was supported in part through funds provided by ERDA under Contract EY-76-C-02-3069.*000, and in part by the A. P. Sloan Foundation.

[1]For a review, see L. Montanet, in Proceedings of the Experimental Meson Spectroscopy Conference, Northeastern University, 1977 (unpublished); CERN Report No. CERN/EP/PHYS 77-22 (unpublished).

[2]A. Chodos, R. L. Jaffe, K. Johnson, C. B. Thorn, and V. F. Weisskopf, Phys. Rev. D 9, 3471 (1974).

[3]E. W. Colglazier and J. L. Rosner, Nucl. Phys. B27, 349 (1971).

[4]A. Dar, M. Kugler, Y. Dothan, and S. Nussinov, Phys. Rev. Lett. 12, 82 (1964).

[5]J. L. Rosner, Phys. Rev. Lett. 21, 950 (1968).

[6]H. Harari, Phys. Rev. Lett. 22, 562 (1969); J. L. Rosner, *ibid.* 22, 689 (1969).

[7]For a discussion see the review of H. Miettinen, in *Antinucleon-Nucleon Interactions*, Proceedings of the Third European Symposium, Stockholm, 1976, edited by G. Ekspong and S. Nilsson (Pergamon, New York, 1977), p. 495.

[8]T. A. DeGrand, R. L. Jaffe, K. Johnson, and J. Kiskis, Phys. Rev. D 12, 2060 (1975).

[9]R. L. Jaffe, Phys. Rev. D 13, 267 (1977); 13, 281 (1977).

[10]DeTar has argued that semiclassical bag calculations which yield multiquark states heavier than dissociation decay channels are signals of short-range repulsion in those channels (Born-Oppenheimer) rather than quantum states of the system. See C. DeTar, Phys. Rev. D 17, 302 (1978); 17, 323 (1978).

[11]R. L. Jaffe and K. Johnson, Phys. Lett. 60B, 201 (1976).

[12]K. Johnson and C. B. Thorn, Phys. Rev. D 13, 1934 (1976).

[13]The first version of the model seems to have been developed by L. Micu, Nucl. Phys. B10, 521 (1969).

[14]For a review, see J. L. Rosner, Phys. Rep. 11C, 189 (1974).

[15]See, for example, G. F. Chew, in *Antinucleon-Nucleon Interactions* (Ref. 7), p. 515.

[16]R. L. Jaffe and K. Johnson, Comments Nucl. Part. Phys. 7, 107 (1977).

[17]Unlike color-electric forces, color-magnetic forces in the bag model are not long range. Instead they fall off much like dipole-dipole forces in free space. (K. Johnson, unpublished).

[18]The color-magnetic forces between QQ and $\overline{QQ}$ are not "turned off" since these pairs remain in the same relative state all along the trajectory.

[19]For a review see H. Harari, in *Properties of the Fundamental Interaction*, edited by A. Zichichi (Academic, New York, 1972).

[20]A. A. Carter *et al.*, Phys. Lett. 67B, 117 (1977).

[21]We would like to thank J. Rosner for pointing out this interpretation and for several valuable discussions on the subject.

[22]T. E. Kalogeropoulos, in *Experimental Meson Spectroscopy*-1974, proceedings of the Fourth International Conference, Boston, edited by D. A. Garelick (AIP, New York, 1974).

[23]L. Gray, P. Hagerty, and T. Kalogeropoulos, Phys. Rev. Lett. 28, 1491 (1971).

[24]The $C(J=l)$ $S=0$ states at 1870 MeV couple very weakly to $N\bar{N}$ and need not be considered (see Table XI).

[25]A. Rogers, report presented at the 1977 Experimental Meson Spectroscopy Conference, Northeastern, 1977 (unpublished).